Crustal magnetism of the Southern Tyrrhenian Sea from aeromagnetic surveys

G. L. PIANGIAMORE[1,2], O. FAGGIONI[2] & M. S. BARBANO[1]

[1]*Dipartimento di Scienze Geologiche, Università di Catania, Corso Italia 55, 95129 Catania, Italy (e-mail: gpiangiamore@yahoo.it)*

[2]*Stazione di Geofisica Marina INGV-Sede di Portovenere, Villa Pezzino, Via Pezzino Basso 2, 19020 Fezzano di Portovenere (SP), Italy*

Abstract: Aeromagnetic data from the Southern Tyrrhenian Sea have been analysed, to remove the contributions of shallow and deep sources to the magnetic anomalies by applying a processing technology that increases the informative potential of the magnetic data acquired by AGIP with great accuracy, uniform distribution and high density. The aeromagnetic anomaly field has been reduced to the bottom topographic surface by the bottom reduction method. Spectral signal analysis has been carried out to separate low- and high-frequency components. The spectral reference field (SRF), obtained from the cotransformation of low frequencies, gives information about deep magnetic structures. The high-frequency components, computed from the difference between the magnetic anomaly field and the SRF, provides the spectral anomaly field (SAF). The bottom reduced magnetic anomaly field is derived by merging the high- and low-frequency bands. The resulting map provides information about geotectonic features in the Southern Tyrrhenian area and shows the effectiveness of the adopted approach over traditional procedures.

The magnetic cartography of Italy and its surrounding seas is made up of the following previous works: (1) the aeromagnetic anomaly map of Italy (AGIP & Servicio Geologico d'Italia (SGN) 1994; scale 1:1 000 000), obtained by processing the same data as used in this work; (2) the shaded relief magnetic anomaly map at sea level (Chiappini *et al.* 2000; scale 1:1 500 000); (3) the aeromagnetic anomaly map of Italy and surveyed provinces, which is the final product of data processing of the old AGIP map after some integrative surveys conducted by Eni Exploration & Production Division in 2000–2001 in collaboration with the Istituto di Geofisica Marina (Eni Exploration–Production Division & IGMar 2002; scale 1:1 500 000).

The aeromagnetic maps (AGIP & SGN 1994; Eni Exploration–Production Division & IGMar 2002) are smoothed by the effect of the data acquisition height with respect to the Chiappini *et al.* (2000) map, the data for which were acquired in marine and ground surveys. The Chiappini *et al.* map was compiled by merging the marine data of the Osservatorio Geofisico Sperimentale (OGS) of Trieste and the ground network records of the Istituto Nazionale di Geofisica e Vulcanologia (INGV), involving many researchers for several years. This long and expensive data patchwork clearly shows differences from the previous layout and a consequent enhancement in signal informative potential.

In this study the problem of smoothing, typical of aeromagnetic maps, is overcome by means of the (bottom reduction method, BTM; Faggioni *et al.* 2001), which reduces the topographic effect in a short time and shows more highly distinct geomagnetic anomalies with a considerable improvement of informative data content. The present procedure is based on a downward continuation to cancel spectral difference caused by the topographic distance between magnetic sources (seamounts and volcanic islands) and survey level so as to better characterize the anomalies.

Main volcanic and structural features

The Southern Tyrrhenian Sea represents a complex Cenozoic oceanic back-arc basin with different areas of extensional deformation as a result of lowering, spreading, subduction and magmatism (Faccenna *et al.* 2004). Its triangular shape is irregular, with the western margin larger than the eastern one. It is delimited on the western side by the Corsica–Sardinia block, on the southern side by Sicily and on the eastern side by the Italian mainland and the Calabrian Arc. The abyssal plain is floored by basaltic crust. Different dynamic processes have generated a volcanism associated with extension and another linked to subduction phenomena, so we find different magmatic volcanic sites: (1) northward the small circular oceanic basins of Magnaghi–Vavilov and Marsili are separated by a north–south trending structural discontinuity; (2) to the SE, the Aeolian Arc with its

From: MORATTI, G. & CHALOUAN, A. (eds) 2006. *Tectonics of the Western Mediterranean and North Africa.* Geological Society, London, Special Publications, **262**, 337–348.
0305-8719/06/$15.00

seven volcanic edifices forms a semicircle offshore from the continental shelf of the Calabrian Arc; (3) Ustica is in a transition zone between two domains, the Tyrrhenian Basin and the Apennine–Maghrebian Chain.

In the Southern Tyrrhenian Sea, because of the greater extension rate than in the northern part, there are more intense magmatic processes and thinned crust. Therefore oceanic crust occurs mostly in the southern sectors of the area (Malinverno & Ryan 1986). The deep-water volcanoes have developed through an incremental growth process. Vavilov and Magnaghi were formed in the Early Pliocene back-arc basin, Marsili dates back to the Mid-Pliocene (Faggioni *et al.* 1995). Aeolian volcanism and Ustica were active from the Early Pleistocene. Furthermore, geological studies and seismic reflection profiles have revealed the presence of approximately NW–SE transcurrent faults in the Southern Tyrrhenian area. The Pleistocene and present-day rise of magmas within the Tyrrhenian domain causes a very high heat flow, reaching average values of 200 mW m^{-2} and a geothermal gradient locally exceeding 100 °C km^{-1} in the Tyrrhenian Sea and its margins (Mongelli *et al.* 1989). Across the Selli Line and the Vavilov–Magnaghi basin, heat flow values are irregular and show a wider range between <100 and >200 mWm^{-2}. This is typical of young rift domains or young oceanic crust–volcanic districts subject to hydrothermal circulation (Della Vedova *et al.* 2000*a, b*). The highest values occur as minor spots within the Vavilov–Magnaghi and Marsili basin and occupy wider sectors across the Campania margin and in the Northern Sicily basin. Crustal thickness decreased from 30 km to about 10 km during middle late Miocene to Pleistocene stretching and then both intrusive and extrusive magmatism became important (Sartori *et al.* 2004).

Input data

The input data used for the bottom reduction method are the following: Southern Tyrrhenian Sea bathymetry (kindly provided by CNR of Bologna, Fig. 1); aeromagnetic data (intensity of total magnetic field F) acquired by AGIP in the late 1970s aeromagnetic surveys (Fig. 2); vertical gradient increase parameters (parameters of vertical projection for frequency bands of the anomaly field: the first parameter is for low frequency, the second for high frequency).

Aeromagnetic surveys

The analysed data come from the aeromagnetic surveys performed by AGIP over the Southern Tyrrhenian Sea in 1977. The flight pattern covers a surface area of 69 173 km^2 and is made up of 230 850 measurements with an average spacing of sampling step of 0.5 km, covering an area approximately between 38° and 41°N and 10° and 15°E.

The surveys are arranged in a grid of lines (L) oriented NE–SW and spaced 5–10 km apart, linked to transverse check tie-lines (T) oriented SE–NW and spaced at an average of 15 and 7.5 km, respectively (Fig. 3). The area has been explored by means of a caesium-vapour magnetometer (0.01 nT sensibility) and reliable flight line positioning systems at a flying height of 2590.80 m above sea level (about 8500 feet) and 1463.04 m above sea level (4800 feet). The regional gradient is 3.232 nT km^{-1} ($\Delta\varphi$) to the north and 0.726 nT km^{-1} to the east ($\Delta\lambda$).

Data processing

The aeromagnetic data have been treated as follows: (1) pre-processing to produce a new database; (2) gridding; (3) systematic error correction; (4) reduction to the International Geomagnetic Reference Field (IGRF); (5) preliminary geomagnetic anomaly map representation; (6) further elaboration of the aeromagnetic anomaly map; (7) production of a definitive version of the magnetic anomaly map 'polished' from the linear trend. All data processing was carried by means of Oasis montaj v5.0 (Geosoft) software. The geographical data were projected into a new cartographic system based on the Transverse Mercator Projection (latitude 0°, longitude 14°, east 1 50 0000 m and false north 0 m), using the WGS84 datum. Accordingly, UTM is used as the projection system for all maps produced in this study. The grid cell size is 3 km, the scale is 1:1 500 000 and illumination has an inclination of 45° and a declination of 45°.

Short-term variations of the geomagnetic field, such as magnetic storms and bays, have been removed from the airborne magnetic data, using a reference base station within the study area. The IGRF is updated every 5 years to take into account the geomagnetic field changes over time. The 1980 epoch is the nearest to the survey one (1977–1979), so the calculated IGRF 1980.0 has been removed from the magnetic relief. The residual contribution, ΔF, is the magnetic field mainly associated with magnetic minerals in crustal rocks. The magnetic anomaly is, in fact, expressed by the relation $\Delta F = F_{obs} - F_{ref}$, where F_{obs} is the observed magnetic field and F_{ref} is the magnetic field computed through the IGRF model. The computed anomaly values on the preliminary aeromagnetic anomaly map are unreliable because at the survey time the reference field was based

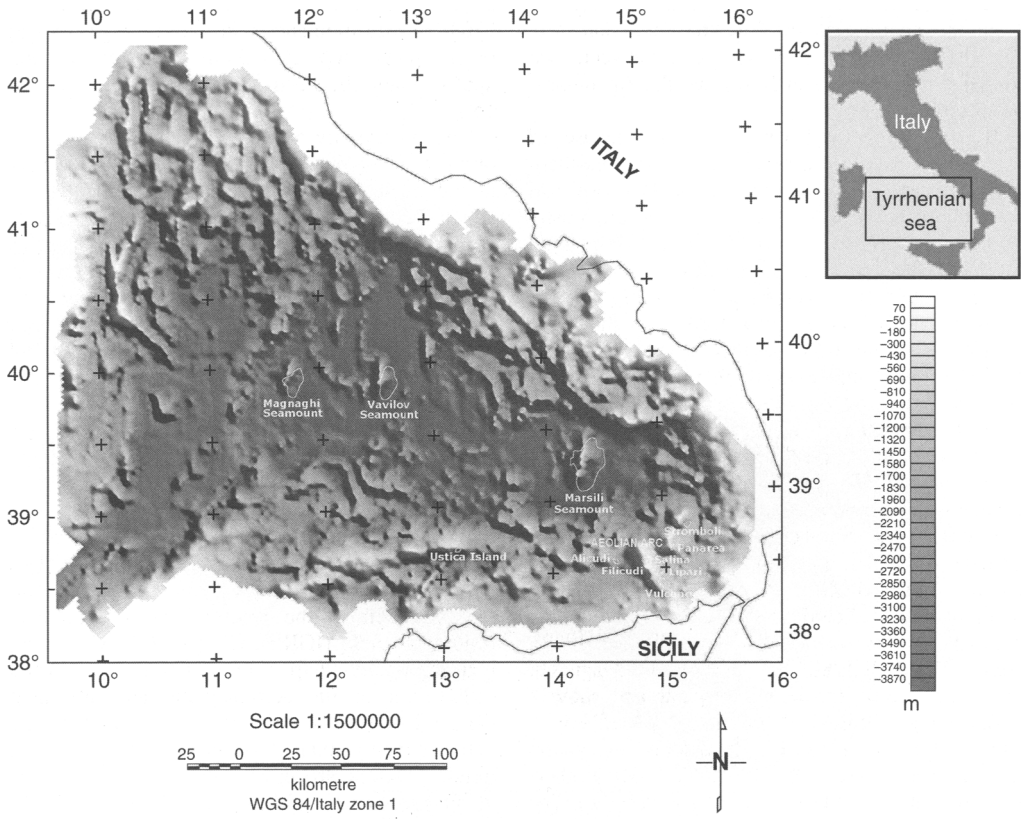

Fig. 1. Grey-scale map, in which the colour saturation from light to dark is modulated by the bathymetry values (shallow areas are the lighttest; deepest areas are the darkest). The greatest depth in the Southern Tyrrhenian Sea is about 4 km.

on a subjective surface made up of a tangle of local planes. Furthermore, the resulting anomaly map shows a shift of some tens of nanotesla with respect to the IGRF field at its composed zero level (Cassano 1984). To define and remove this difference in the reference field, the most representative geomagnetic profile in the area has been used. The procedure to remove this subjective surface contribution is as follows: a north–south-oriented profile on the reduced map has been selected (see Fig. 3 for profile location); the values extracted along the corresponding grid points have been visualized in a diagram (Fig. 4); the mean (−71 nT) between the two nearest points to the inflexion below the peak value (−62.7 and −79.7 nT) has been subtracted from the geomagnetic anomaly field values (Piangiamore 2005).

The inflexion indicates the most significant reference value to define the anomaly area and it has been assumed as a reference correction value. This procedure implies an approximation, because the compensation parameter is computed by a profile and extended to the entire area examined, but this approximation is negligible in regional studies.

Now the geomagnetic anomaly values are acceptable and the aeromagnetic anomaly map appears 'cleaned' from linear trend (Fig. 5).

A new residual aeromagnetic anomaly map in the Southern Tyrrhenian region

The reprocessed aeromagnetic anomaly map of the Southern Tyrrhenian Sea defines with precision an area that is characterized by high-frequency anomalies that can be associated with local volcanic features. Some magnetic anomalies are well isolated from the regional background and assume a strictly dipolar shape. The negative magnetic signature of the Tyrrhenian domain is caused by the high heat flow and geothermal gradient observed in this area (Mongelli *et al.* 1989), which demagnetizes crust above the 580 °C isotherm. The relative strong negative values reach −350 nT, characterizing the sea

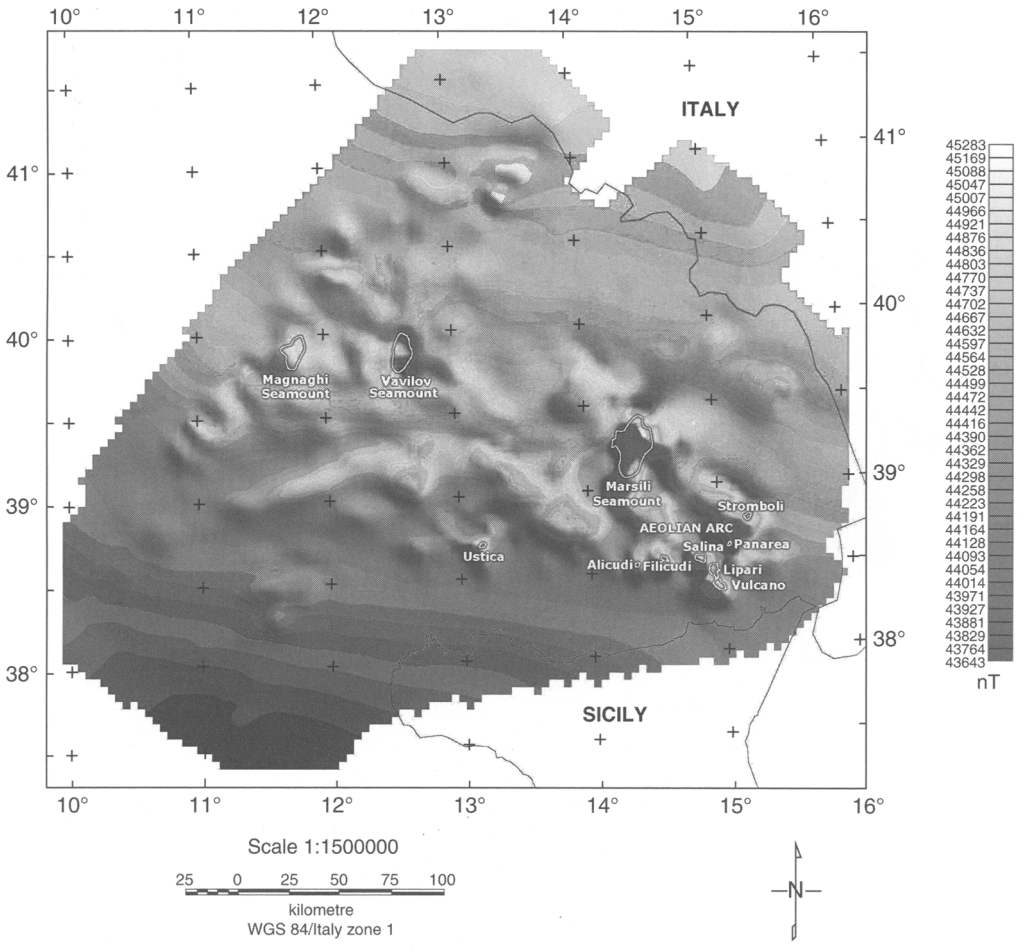

Fig. 2. Total geomagnetic field map of the Southern Tyrrhenian Sea.

bottom, whereas the magnetic values rapidly increase generally corresponding to seamounts and volcanic islands. Finally, the values decrease again to slightly negative near the Tyrrhenian margin with its large regional amplitude anomalies (up to 100 nT less than in the southwestern Tyrrhenian sector offshore). This area corresponds to the shelf and the continental margin of the northern Sicilian coast, and is due mainly to the contact between oceanic and continental crust. The seamounts match high-frequency anomaly zones. The interpretation of these magnetic features as submarine volcanic manifestations is also supported by the following evidence.

(1) Heat flow and magnetic anomalies are elevated in the Southern Tyrrhenian Sea (Della Vedova *et al.* 2000).

(2) Metal-rich sediments near the Messinian–Pliocene boundary (Robertson 1990) may have been produced by coeval hydrothermal circulation triggered by the shallow intrusions.

(3) The Moho is almost flat regionally, around a mean value of 10 km in the Magnaghi and Marsili basins where the lithospheric mantle also seems to be very thin (Panza *et al.* 2004); whereas it increases to 15 km in the Southern Tyrrhenian margin. Moreover, the very wide area with the Moho at shallow depth includes not only the inferred oceanic crust but also the lower and middle Sardinia continental margin.

Signal analysis

The magnetic signal depends on the size, shape, depth of occurrence and magnetization of the source body. Magnetic anomalies generally arise from source bodies at significantly different depth levels.

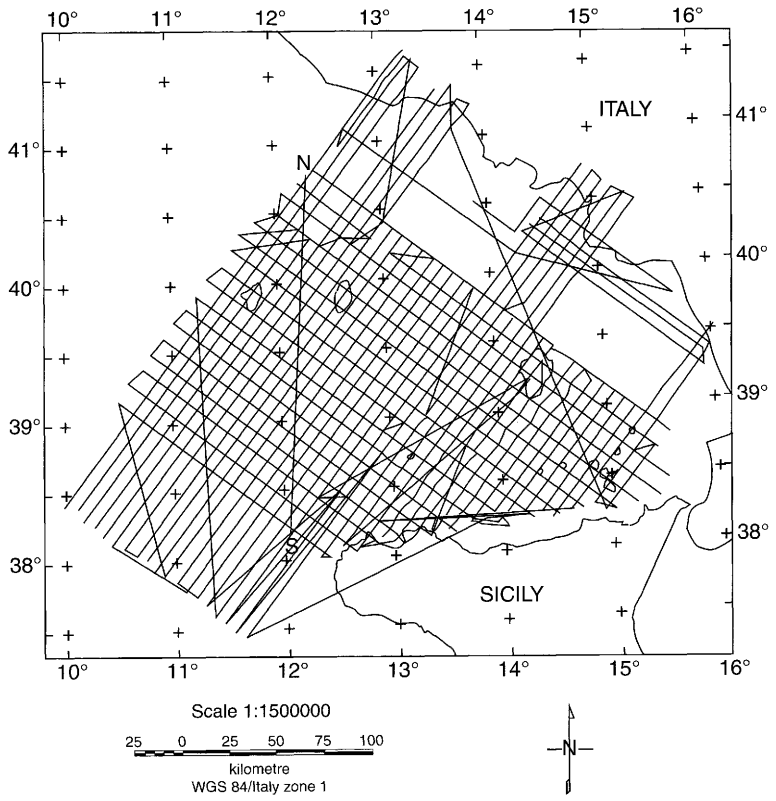

Fig. 3. Aeromagnetic track lines and north–south profile analysed in the Figure 4 and used to remove the linear trend from aeromagnetic anomaly values.

A filtering procedure is used to separate anomalies by their wavelengths as well as to enhance high-frequency (short-wavelength) residual components of the observed potential field by attenuating the dominant regional components and suppressing regular and random noise. Residual-regional anomaly separation by filtering is based on the assumption that a given geological source energy is attenuated more rapidly at high spatial frequencies (short wavelengths) than at low spatial frequencies (long wavelengths) as the source depth increases. The radially averaged power spectrum is a logarithmic plot of the Fourier transformed gridded magnetic data, representing the power

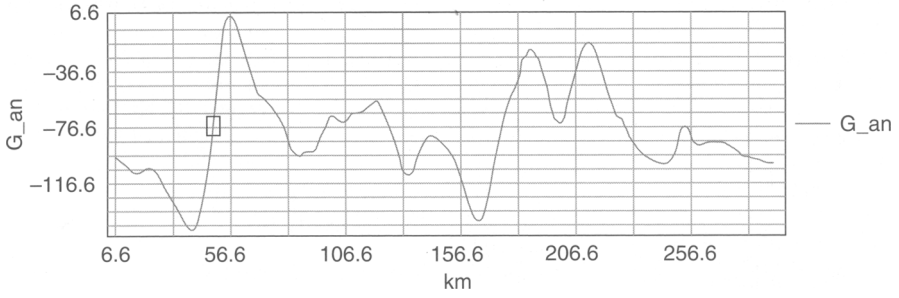

Fig. 4. North–south profile selected to correct anomaly data. The ground units in metres are represented on the *x*-axis, and the values extracted from the grid of anomaly data in units of nT on the *y*-axis.

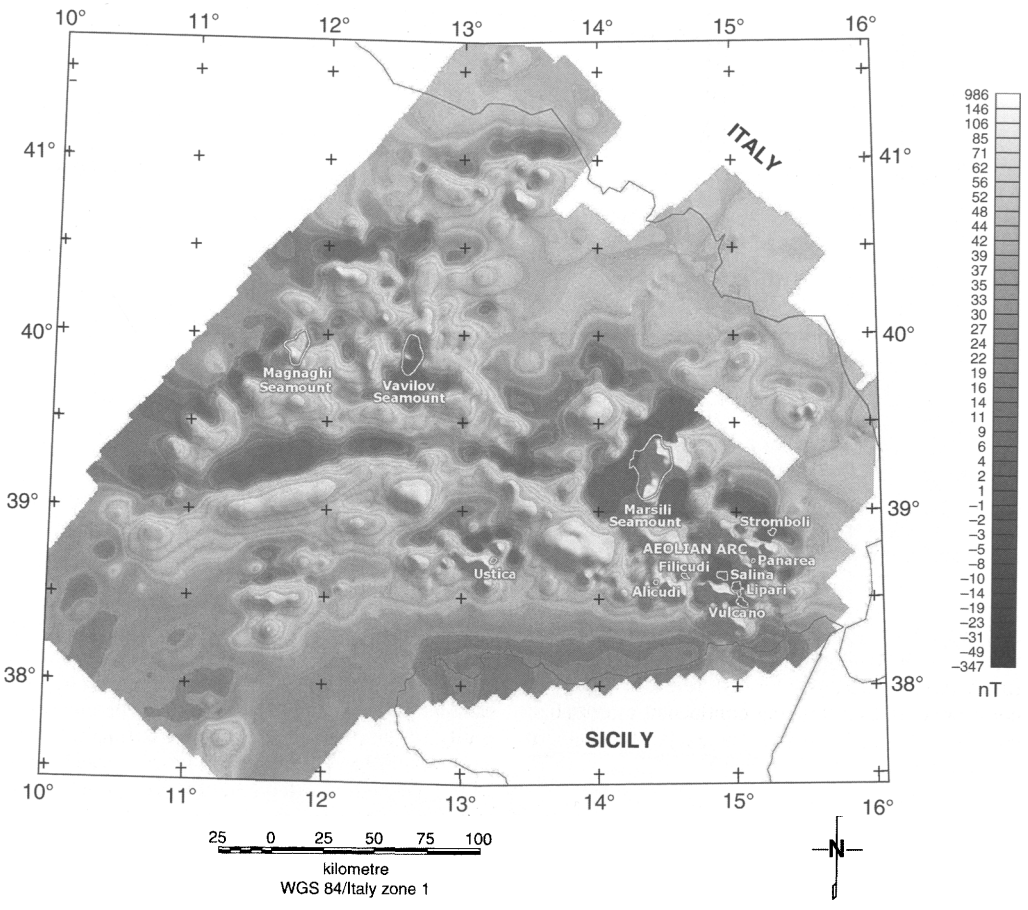

Fig. 5. The reprocessed aeromagnetic anomaly map of the Southern Tyrrhenian Sea after spurious trend removal.

logarithm, which is equal to the square of spectral amplitude. It represents the spectral energy content in all surface directions, being obtained by integrating each radial frequency component over all azimuths. The spectrum is a statistical estimate of the average frequency bands over the area.

The power spectrum exhibits a distinct slope (Fig. 6) that provides the intercept parameter for the evaluation of cut-off wavelength. It shows an amplitude decay at the wavelength λ of 90 km corresponding to a cut-off wavenumber of 0.01 cycles km^{-1}. It is assumed that the decay of the power spectrum curve may be approximated by linear slopes (gradients) associated with ensembles of magnetic sources located at different depths. Applying a 2D fast Fourier transform (FFT) filter created on this cut-off wavelength to the gridded aeromagnetic anomaly, different depth sources are separated. The low-pass filter used with 90 km cut-off wavelength value retains all wavelengths larger than 90 km and rejects all wavelengths smaller than 90 km. High-frequency (short-wavelength) components of the observed potential fields originate from relatively shallow magnetic sources, whereas low-frequency components derive from deep sources.

Spectral reference field

A low-pass filter map at a cut-off wavenumber of 0.01 cycles km^{-1} is the graphical representation of the spectral reference field (SRF) and it gives information about deep magnetic structures with long wavelength. The anomaly pattern, after low-pass filtering, tends to accentuate anomalies caused by deep sources at the expense of anomalies caused by small and shallow sources (typically volcanoes or intrusive bodies). Low-amplitude anomalies usually indicate basement block structures (e.g. uplifts, horsts). The computed

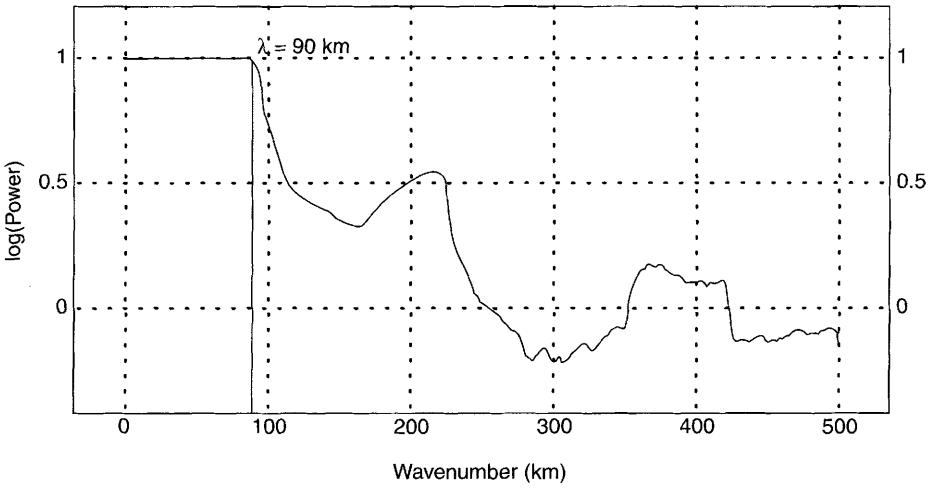

Fig. 6. Radially averaged power spectrum. The energy (power) of the observed data components is presented on a logarithmic scale. The horizontal axis represents wavenumber values in cycles per ground units (km); the cut-off wavelength $\lambda = 90$ km.

SRF map (Fig. 7) shows a minimum magnetic pattern separating the two great Southern Tyrrhenian basins (the Vavilov and Marsili basins). It is a narrow zone corresponding to a thinning continental crust called the 'Issel Bridge', which crosses Issel Seamount (Sartori 2003) (see the next map).

Spectral anomaly field

Anomaly separation is a processing method used to reveal shallow subsurface source distributions, which are often the main target of magnetic exploration. A high-frequency map has been obtained by subtracting the contribution of the SRF from the reprocessed aeromagnetic anomaly data. The result is the spectral anomaly field (SAF), which highlights shallow magnetic sources that are related to short wavelengths (Fig. 8). This map amplifies our knowledge about superficial magnetic structures, showing in detail the geomagnetic characteristics of all seamounts of the Southern Tyrrhenian area. Complex and intense short-wavelength anomalies, caused by volcanic edifices arising from crustal thinning and effusive events, are plainly evident. Magnetic anomalies clearly correspond to the emerged volcanoes (such as the Aeolian Arc and Ustica Island); some are major seamounts (Marsili, Magnaghi) and some minor ones (such as De Marchi, Flavio Gioia, Glauco, Sisifo, Aceste, Anchise, Prometeo, Enarete, Eolo and Lamentini). The Vavilov and Farfalla Seamounts and some Aeolian Arc volcanic areas show strongly negative anomalies; this is very unusual for crustal magmatic bodies, which are potentially highly magnetic (Arisi Rota & Fichera 1987). The Secchi, Sirene and Issel Seamounts magnetic anomaly are negative, too, but less than the previous seamounts. Various hypotheses can be formulated to justify the apparent incongruity of the presence of negative anomalies in an area rich in lower continental crust, oceanic crust and upper mantle, which are usually strongly magnetic: (1) demagnetization of the rocks as a result of the Curie temperature being exceeded, as this is a zone of elevated heat flow (the Moho is at about 10 km depth in the Vavilov and Marsili basins (Scrocca *et al.* 2003); (2) intense tectonization with consequent rock fracture and cataclasis favouring rock alteration and the oxidation of magnetite, eventually to other oxides (hematite, goethite); (3) hydrothermal alteration, which occurs particularly in geochemical environments with gas leaks (Etiope *et al.* 1999).

Application of the bottom reduction method (BTM) to analysis of aeromagnetic data

The intensity of the geomagnetic field is distorted by the topographic effect, especially in highly magnetic volcanic rocks. Geomagnetic anomaly field intensity strongly decreases with increasing depth. In magnetic interpretation it is referred to as the 'continuation concept', as the magnetic anomalies become broader (exhibiting lower frequency content) when the distance between the source of anomaly and magnetometer sensor increases. Moreover, the topographic compensation tends to flatten out the amplitude differences of high- and

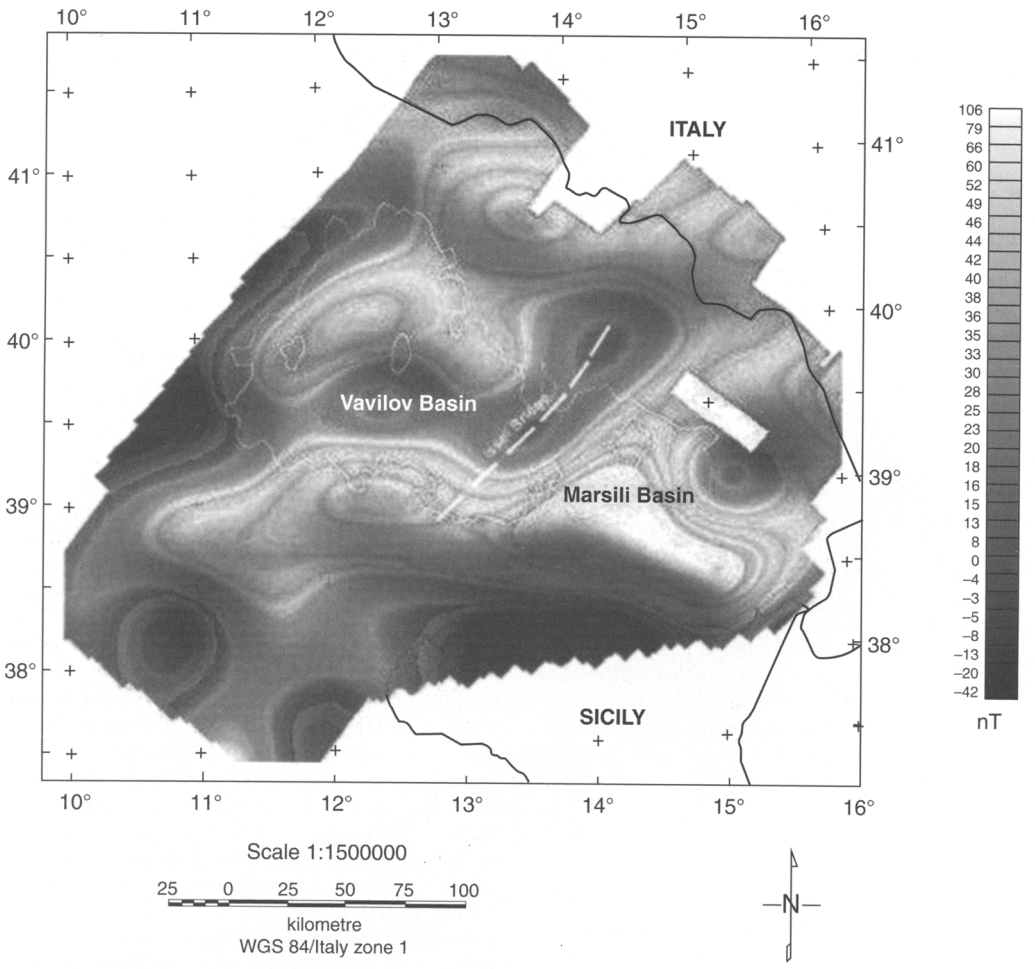

Fig. 7. Spectral reference field (SRF): low-pass component of IGRF anomaly field. The Issel Bridge is indicated by the white dashed line.

low-frequency components. The topographic reduction to the aeromagnetic anomaly field of the Southern Tyrrhenian Sea has been performed, by means of the Bottom Reduction Method (BTM) by Faggioni *et al.* (2001). This technique provides a rapid and straightforward method to process data so as to reduce the distortions of the geomagnetic anomaly field caused by the sea bottom morphology and corresponding variation of the sensor–sea bottom distance. The aim of BTM is to discriminate, in a simple and efficient way and with the highest possible definition, the high-frequency spatial anomaly field, often associated with seamounts and volcanic islands, from the low-frequency crustal structure, regardless of the depth of the sea bottom topography. The Tyrrhenian structural setting is characterized by variable bathymetry. The BTM is based on the downward continuation of the spectral high- and low-frequency bands, in accordance with their own vertical gradient. The data are projected over the topographic surface according to the following formula:

$$\Delta F^{\mathrm{L,H}}_{\mathrm{BTM}}(\varphi, \lambda) \equiv \Delta F^{\mathrm{L,H}}(\varphi, \lambda) + \frac{1}{2} d(\varphi, \lambda) K^{\mathrm{L,H}} \frac{\Delta F^{\mathrm{L,H}}(\varphi, \lambda)}{|\Delta F^{\mathrm{L,H}}_{\mathrm{max}}|}$$

where φ and λ are the geographical coordinates of array points; $\Delta F^{\mathrm{L,H}}_{c}(\varphi, \lambda)$ is the low- (high)-frequency BTM corrected intensity of geomagnetic field anomaly; $\Delta F^{\mathrm{L,H}}(\varphi, \lambda)$ is the low- (high)-frequency intensity of sea-level geomagnetic field anomaly; $d(\varphi, \lambda)$ is the bathymetric depth; $K^{\mathrm{L,H}}$ is

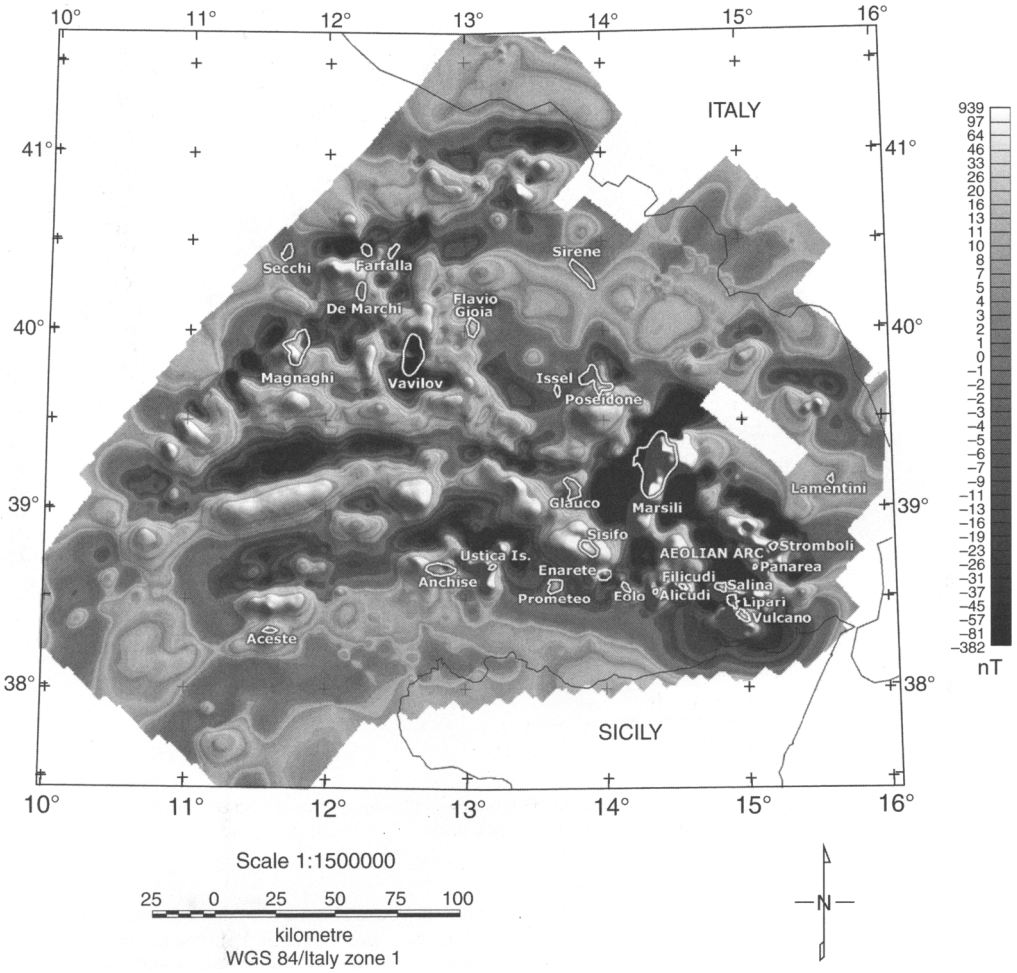

Fig. 8. Spectral anomaly field (SAF): high-pass component of the IGRF anomaly field. The Southern Tyrrhenian seamounts are indicated.

the low- (high)-frequency vertical increment coefficient; $\Delta F^{L,H}_{max}$ (φ, λ) is the low- (high)-frequency maximum intensity of the sea-level anomaly.

This metrological technique allows us to spread the magnetic data values, measured at a certain altitude over the topographic surface, varying the depth by means of low-frequency band vertical increment gradient K^L for the correction of low-frequency band anomaly field component and high-frequency band vertical increment gradient K^H for the correction of the high-frequency one. The values of K for each of the spectral bands can be computed in an empirical way. The assumption that the continuation has different behaviour according to the frequency bands is respected by using different vertical gradients for the high- and low-frequency bands. This procedure allows us to recalculate the observed potential field at the sea bottom surface beneath the plane of measurements. It enhances short-wavelength (high-frequency) components of the potential field, which are generated by relatively shallower sources. Reduction involves the following steps: (1) transform matrix of magnetic values to the frequency domain; (2) carry out spectral analysis of data and search for frequency of classification (cut frequency) to separate high (H) and low (L) bands; (3) co-transform low frequencies to obtain the spectral reference field (SRF); (4) compute the anomaly field high-frequency band to obtain the spectral anomaly field (SAF) by subtraction from the IGRF anomaly field of the SRF; (5) make a vertical projection of SRF and SAF to the sea bottom by means of the K^L (LF band vertical gradient and the K^H (HF band vertical

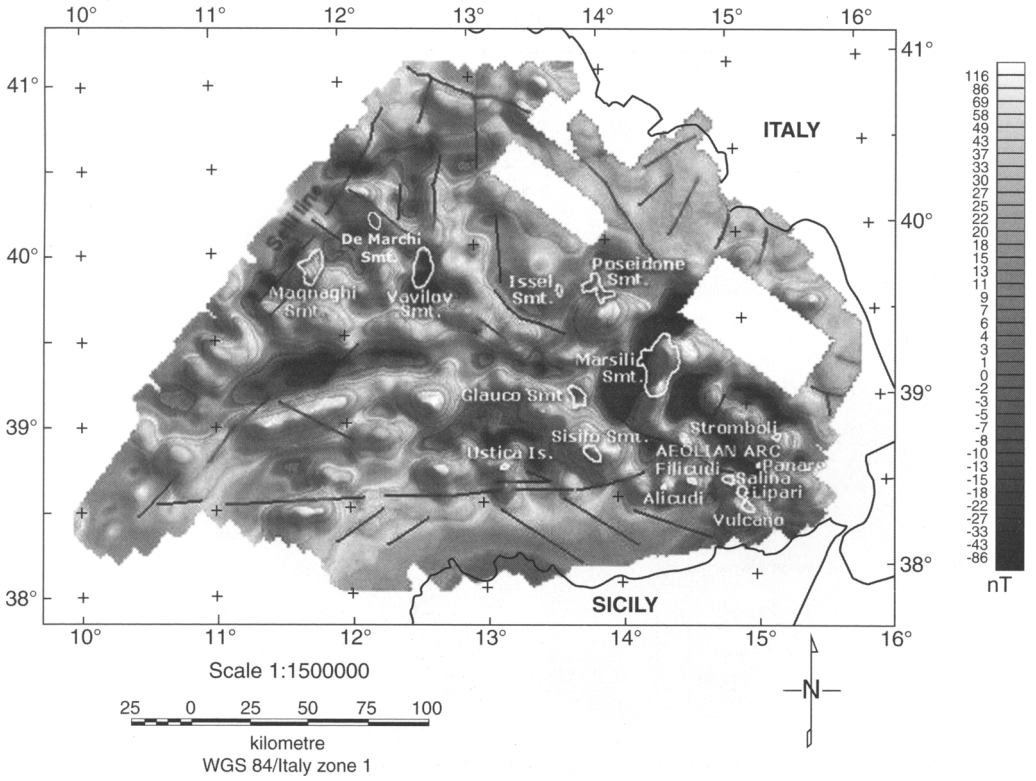

Fig. 9. BTM map of the Southern Tyrrhenian Sea: IGRF anomaly field projected to sea bottom. Tectonic lineaments redrawn from Mattei *et al.* (2004) are shown by the bold black lines.

gradient); (6) merge subsets of frequency to obtain bottom reduced magnetic anomaly field (BTM).

The definitive and 'corrected' aeromagnetic anomaly dataset is processed using an FFT. The power spectrum is analysed to delineate an appropriate cut frequency, to separate the magnetic effects of deep subsurface sources from shallow ones. To achieve an efficient merging, the low- and high-frequency components of the geomagnetic field are isolated and projected over the topographic surface by means of differentiated vertical gradients for the two bands: $K^{L} = 55\ \mathrm{nT\,km^{-1}}$ for the low-frequency band; $K^{H} = 72\ \mathrm{nT\,km^{-1}}$ for the high-frequency one. These coefficients, calculated in the central and northern Tyrrhenian Sea, are extended to the southern zone, because the differences in vertical gradients, caused by the inductive field latitude variations, are not significant at our scale of investigation (Faggioni *et al.* 1995, 2001). The style of the anomaly field is defined by shape and susceptibility of the natural crustal sources.

The BTM corrected anomaly map is then synthesized by merging the BTM corrected SAF and BTM corrected SRF. To apply the BTM formula, three database channels are necessary: geographical reference, geomagnetic anomaly intensity and depth. Thus, the magnetometric and the bathymetric databases have been linked, digitizing the line-path grid anomaly values over the topography values. At this point the data are ready to be filtered and BTM processed.

Figure 9 shows the BTM map of the Southern Tyrrhenian area. The improvement of the information potential of the geomagnetic signal is mainly due to the enhancement of the large wavelength anomalies, which are otherwise suppressed by other projection methods. The BTM procedure has emphasized some deep sources, without increasing the high-frequency noise too much. The high-frequency noise, typical of standard projection techniques, does not affect the procedure, which is more stable and shows a meaningful signal increase. This approach has allowed us to obtain a better definition of the geomagnetic signals even when applied to a large area with a strong horizontal gradient of depth and magnetic field intensity. The BTM map emphasizes geomagnetic anomalies described so far and highlights a field of relatively strong anomalies

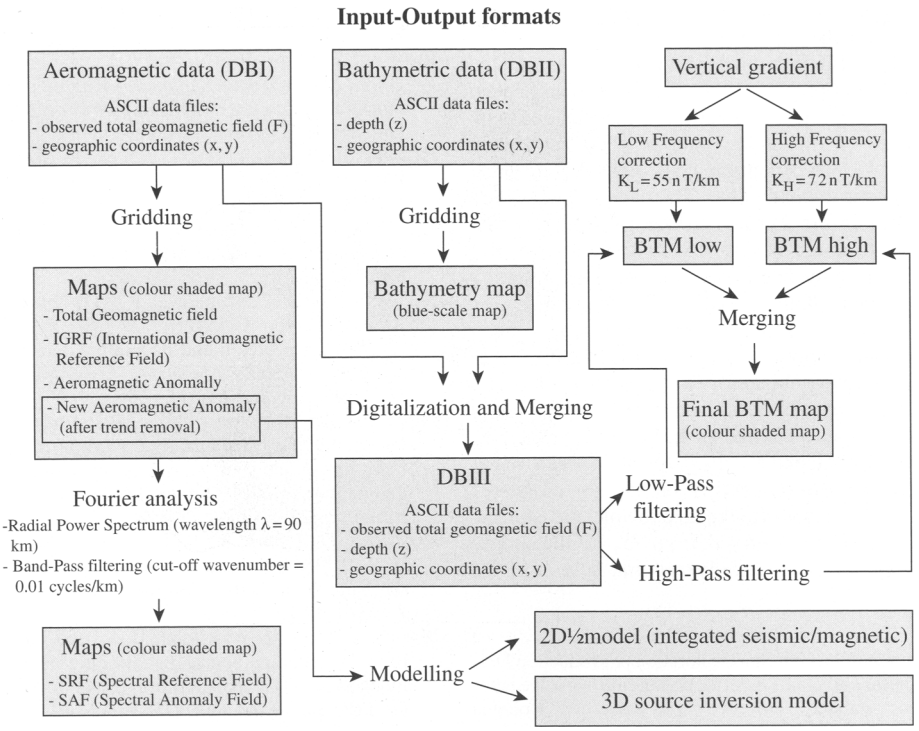

Fig. 10. Flow-chart explaining the data-processing and signal analysis steps.

confined between the Selli Line and the De Marchi Seamount. The moderate positive magnetic anomaly associated with the Campania margin and the long wavelength modest negative anomaly, trending west–east across the North Sicily Basin, shows a geomagnetic field style characterized by low intensity and low horizontal gradient, typical of continental crust geomagnetic field.

All the methods, phases of work and procedures that have been used to produce the final map layout are schematically summarized in the flow-chart shown in Figure 10.

Conclusions

The aeromagnetic anomaly map of Southern Tyrrhenian area has been reprocessed. It gives an unprecedented view of the magnetic signature of the major tectonic elements in their regional setting in comparison with the previously available compilations.

The spectral reference field (SRF) map, obtained by low-pass filtering of the reprocessed aeromagnetic anomaly data, shows the contribution of deep magnetic sources with long wavelength, without the effect of superficial anomalies, which in the Southern Tyrrhenian Sea are typically seamounts and submarine lava flow (such as Prometeo). The most important evidence in the SRF map is the minimum magnetic pattern separating the Vavilov–Magnaghi basin from Marsili one. In this area the edge of thinning continental crust called the 'Issel Bridge' is located.

The spectral anomaly field (SAF) map, obtained by subtracting the SRF contribution from the anomaly field, highlights the shallow subsurface sources. The SAF map provides a detailed picture of the geomagnetic characteristics of all the seamounts (Marsili, Vavilov, Magnaghi, Secchi, Farfalla, De Marchi, Flavio Gioia, Sirene, Issel, Poseidone, Glauco, Sisifo, Lamentini, Aceste, Anchise, Prometeo, Enarete, Eolo) and volcanic islands (the Aeolian Arc and Ustica Island) of the Southern Tyrrhenian area. Almost all volcanoes are highly magnetic, except for Vavilov and Farfalla seamounts (and other restricted volcanic areas, such as in the Aeolian Arc), which have a highly negative magnetic signature.

The sea-bed reduction of the geomagnetic anomaly field of the Southern Tyrrhenian Sea has been carried out using the bottom reduction method, which is based on downward continuation to cancel spectral differences caused by the distance

between magnetic sources (seamounts and volcanic islands) and the survey level.

A shaded relief map showing the integrated anomaly field projected over the Tyrrhenian Seabed provides a regional-scale view of the crustal magnetic anomalies of the area. There is good correlation between known structural geological features and the magnetic anomaly field. The pattern of magnetic anomalies in the Tyrrhenian Sea is similar to that of other back-arc basins worldwide, and does not show clear spreading-type lineation. The generally low magnetic field values of the Tyrrhenian Sea bottom are dominated by short-wavelength positive–negative anomaly couplets centred over volcanic or intrusive bodies. The strongest magnetic anomalies across the Marsili and Vavilov–Magnaghi basins are roughly centred on the largest seamounts of the area (Marsili and Magnaghi positive and Vavilov negative) or on subcircular or slightly elongated sea-floor elevations often related to volcanic edifices.

The BTM map derived from the AGIP survey could be used for detailed structural studies in the Tyrrhenian Sea.

We are grateful to Eni Spa Exploration & Production Division (particularly to I. Giori) for permission to use the aeromagnetic dataset, and to CNR–Ismar of Bologna (especially M. Marani) for kindly providing the Southern Tyrrhenian Sea bathymetry. The authors wish to thank A. Casas and J. W. Jones for their careful reviews and useful suggestions that improved the manuscript. The first author wishes to dedicate this paper to Giuseppe.

References

AGIP S.P.A. & SERVIZIO GEOLOGICO D'ITALIA 1994. *Aeromagnetic map of Italy at 1:1 000 000 scale*. Istituto Poligrafico e Zecca dello Stato, Rome.

ARISI ROTA, F. & FICHERA, R. 1987. Magnetic interpretation related to geo-magnetic provinces. The Italian case history. *Tectonophysics*, **38**, 179–196.

CASSANO, E. 1984. Rilievi magnetici per la ricerca mineraria. *Atti del primo convegno di geomagnetismo (INGV)*, 117–163.

CHIAPPINI, M., MELONI, A., BOSCHI, E., FAGGIONI, O., BEVERINI, N., CARMISCIANO, C. & MARSON, I. 2000. Shaded relief magnetic anomaly map of Italy and surrounding marine areas. *Annali di Geofisica*, **43**(5), 983–989.

DELLA VEDOVA, B., BELLINI, S., PELLIS, G. & SQUARCI, P. 2000*a*. Deep temperatures and surface heat-flow distribution. *In*: VAI, G. B. & MARTINI, L. P. (eds) *Anatomy of an Orogen: the Apennines and Adjacent Mediterranean Basins*. Kluwer, Dordrecht, 65–76.

DELLA VEDOVA, B., BELLINI, S., PELLIS, G. & SQUARCI, P. 2000*b*. Heat flow map of Italy and surrounding seas with the main factors influencing surface heat flow distribution. *In*: VAI, G. B. & MARTINI, L. P. (eds) *Anatomy of an Orogen: the Apennines and Adjacent Mediterranean Basins*. Kluwer, Dordrecht.

ENI EXPLORATION–PRODUCTION DIVISION & IGMAR 2002. *Aeromagnetic Anomaly Map of Italy and Surveyed Provinces*. Eni Exploration-Production Division R&D Project, Milan.

ETIOPE, G., BENEDUCE, P., CALCARA, M., FAVALI, P., FRUGONI, F., SCHIATTARELLA, M. & SMRIGLIO, G. 1999. Structural pattern and CO–CH degassing of Ustica Island, Southern Tyrrhenian basin. *Journal of Volcanology and Geothermal Research*, **88**, 291–304.

FACCENNA, C., FUNICIELLO, F., PIROMALLO, C., ROSSETTI, F., GIARDINI, D. & FUNICIELLO, R. 2004. Subduction and back-arc extension in the Tyrrhenian Sea. *Memorie Descrittive Carta Geologica d'Italia*, **44**, 165–184.

FAGGIONI, O., BEVERINI, N., CARMISCIANO, C. & GIORI, I. 2001. A metrologic method of anomaly field amplitude bottom reduction undersampled geomagnetic marine surveys. *Marine Geophysical Research*, **22**, 63–79.

FAGGIONI, O., PINNA, E., SAVELLI, C. & SCHREIDER, A. A. 1995. Geomagnetism and age study of Tyrrhenian seamounts. *International Geophysical Journal*, **123**, 915–930.

MALINVERNO, A. & RYAN, W. B. F. 1986. Extension in the Tyrrhenian Sea and shortening in the Apennines as result of arc migration driven by sinking of the lithosphere. *Tectonics*, **5**(2), 227–245.

MATTEI, M., D'AGOSTINO, N., FACCENNA, C., PIROMALLO, C. & ROSSETTI, F. 2004. Some remarks on the geodynamics of the Italian region. *Periodico di Mineralogia, Special Issue 1: A Showcase of the Italian Research in Petrology: Magmatism in Italy*, **73**, 7–27.

PANZA, G. E., PONTEVIVO, A., SARAÒ, A., AOUDIA, A. & PECCERILLO, A. 2004. Structure of the lithosphere–asthenosphere and volcanism in the Tyrrhenian Sea and surroundings. (Struttura della litosfera–astenosfera e vulcanismo nel Mar Tirreno e regioni adiacenti.) *Memorie Descrittive della Carta Geologica d'Italia*, **44**, 29–56.

PIANGIAMORE, G. L. 2005. *Geomagnetic anomaly in basin opening structures: the Tyrrhenian Sea example*. PhD thesis, University of Catania, Italy.

ROBERTSON, A. H. F. 1990. Pliocene basal dolomitic and Fe–Mn sediments from the Tyrrhenian Sea, western Mediterranean, Leg 107. *In*: KASTENS, K. A., MASCLE J., *ET AL.* (eds) *Proceedings of the Ocean Drilling Program, Scientific Results, 107*. Ocean Drilling Program, College Station, TX, 129–140.

SARTORI, R. 2003. The Tyrrhenian back-arc basin and subduction of the Ionian lithosphere. *Episodes*, **26**(3), 217–221.

SARTORI, R., TORELLI, L., ZITELLINI, N., CARRARA, G., MAGALDIA, M. & MUSSONIA, P. 2004. Crustal features along a W–E Tyrrhenian transect from Sardinia to Campania margins (Central Mediterranean). *Tectonophysics*, **383**, 171–192.

SCROCCA, D., DOGLIONI, C. & INNOCENTI, F. 2003. Contraints for an interpretation of the Italian geodynamics: a review. *Memorie Descrittive della Carta Geologica d'Italia*, **62**, 15–46.